NASA Technical Memorandum 86225

8.3 and 12.4 Micron Imaging of the Galactic Center Source Complex with the Goddard Infrared Array Camera

D. Y. Gezari, R. Tresch-Fienberg,
G. G. Fazio, W. F. Hoffman, I. Gatley,
G. Lamb, P. Shu and C. McCreight

JULY 1985

NASA

NASA Technical Memorandum 86225

8.3 and 12.4 Micron Imaging of the Galactic Center Source Complex with the Goddard Infrared Array Camera

D. Y. Gezari, G. Lamb* and P. Shu*
NASA/Goddard Space Flight Center

R. Tresch-Fienberg*, and G. G. Fazio*
Harvard-Smithsonian Center for Astrophysics

W. F. Hoffman
Steward Observatory, University of Arizona

I. Gatley
United Kingdom Infrared Telescope

C. McCreight*
NASA/Ames Research Center

*Visiting Astronomer at the Infrared Telescope Facility, which is operated by the University of Hawaii under contract from the National Aeronautics and Space Administration.

National Aeronautics and
Space Administration

Goddard Space Flight Center

1985

I. INTRODUCTION

Evidence is accumulating which suggests the presence of a massive luminous object at the Galactic Center. Early high spatial resolution infrared observations of the region (Rieke and Low 1973; Becklin and Neugebauer 1975) revealed a curved ridge of extended 10μm emission containing several bright compact sources, and a larger number of 2μm sources both on and off the ridge including IRS 16 at the position of the point-like non-thermal radio source Sgr A* identified as the nominal Galactic Center (Balick and Brown 1974; Lo 1982). 30-100μm observations suggest that a gas- and dust-depleted region several parsecs in diameter centered on Sgr A* is swept clean by a central luminosity source which powers the far-infrared emission (Becklin, Gatley, and Werner 1982). Reviews by Gatley and Becklin (1981) and Brown and Liszt (1984) discuss the possible role of a central object in explaining the energetics of the innermost few parsecs and the surrounding region of diameter $\sim$ 100 pc.

A ring of neutral gas with inner radius $\sim$ 2 pc encircling the Galactic Center was first inferred from far infrared observations (Becklin, Gatley, and Werner 1982), and later from observations of radio continuum emission (Eckers et al. 1983, Lo and Claussen 1983), infrared fine-structure lines (Genzel et al. 1985), and molecular hydrogen lines (Gatley et al. 1984). Lo and Claussen (1983) suggested that matter may be falling in toward the nucleus from the ring and accreting onto a central object. The kinematics of the complex requires more mass interior to the ring than can be accounted for by the observed infrared stars (Brown and Liszt 1984; Crawford et al. 1985). Observed NeII velocities associated with the infrared sources and the radio continuum emission features can be explained by the presence of a M $\sim$ few times 10^6 $M_\odot$ object at or near IRS 16 (Lacy et al. 1980; Serabyn and Lacy 1985). X-ray emission (Watson et al. 1981), γ-ray emission (Lingenfelter and Ramaty 1982), and extremely broad He I line emission suggesting outflow from IRS 16 (Hall, Kleinmann and Scoville 1982; Geballe et al. 1984; Krisciunas et al. 1984) all are consistent with the "central engine" model.

An alternate model, in which active star formation contributes significantly to the energetics of the innermost few parsecs of the Galactic Center complex, is supported by the large number of supergiant stars observed in the region at 2μm (Lebofsky, Rieke, and Tokunaga 1982), and by the suggestion that the 10μm sources are HII regions heated by imbedded luminosity sources (Becklin et al. 1978a; Rieke and Lebofsky 1979). Lo and Claussen (1983) and Crawford et al. (1985) content that the variety of phenomena observed in the region can not be accounted for by a single large-scale process or event.

The spatially accurate photometry presented here is used to derive detailed color temperature and column density distributions of the 10μm IRS sources and the extended emission in the central parsec. The relationship of these results to the large scale structures and organized material flows in the region, and the implications for the central engine hypothesis, are discussed.

II. INSTRUMENTATION

a) Array Camera Description

The Goddard array camera contains an Aerojet ElectroSystems Co. 16 x 16 pixel Si:Bi AMCID (bismuth doped silicon accumulation mode charge injection device) monolithic array detector with 254 active pixels. The characteristics and performance of Si:Bi AMCID array detectors have been discussed in general by Parry (1980, 1983), McCreight and Goebel (1981), and McKelvey et al. (1985). A detailed description of the 16 x 16 array camera system used here is also given by Lamb et al. (1984).

The array detector, cryogenic MOSFET preamplifiers, optics, and filter wheel mechanisms are mounted in a liquid helium dewar and operated at a temperature of approximately 10K. Two filter wheels contain a variety of interference filters and blocking filters. Anti-reflection coated germanium field and relay lenses demagnify the image to match the diameter of the first Airy diffraction ring to 2 detector pixels at 10μm. The center-to-center distance between detector pixels is 0.2mm.

Sixteen parallel channels of signal processing electronics each contain a preamplifier, correlated double sampler, and 12-bit analog-to-digital converter. A first-in first-out (FIFO) memory feeds two Motorola 68000 microprocessors which generate the 16 x 16 element image "frames" at a typical operating rate of 800 Hz. These images are sorted and co-added separately at each chopper sky position for typical integrations of 60 seconds. The final summed images are down-loaded to an LSI 11/23 microcomputer for background subtraction, flat-fielding and other array arithmetic operations. The microprocessors also commands telescope beam switching during the observations.

b) Detector System Characteristics

The array detector system performance characteristics are summarized in Table 1. AMCID detector sensitivity and noise characteristics are functions of detector operating temperature, read and store voltages, sampling frequency, chopping frequency, and wavelength and intensity of incident illumination. A discussion of these relationships and detailed analysis of the detector system performance characteristics is given by Lamb et al. (1984).

The array detector responsivity was approximately 0.5 amp W^{-1} based on observations of infrared standard stars, about a factor of 10 lower than the responsivity of an ideal system (cf. McCreight and Goebel 1981) and attributable to the low quantum efficiency of this particular device ($\lesssim$5% between 8 and 13μm; this array was an early developmental prototype and is not characteristic of the best performance of its type). The cryogenic MOSFET preamplifiers presently used have voltage noise of about 80 nV $Hz^{-1/2}$ at 1 kHz. MOSFET noise is minimized by choosing an appropriate sampling rate. Charge accumulated at the $\sim$ 2.5 pF input capacitance of the MOSFET yields about a 60 nanovolt signal per electron. The detector well capacity, which affects noise performance and dynamic range, is about 10^5 electrons. At low background, detector dark current limited noise equivalent power (NEP) for this generation of Aerojet arrays (neglecting readout noise) is as low as a few times 10^{-17} W $Hz^{-1/2}$.

Table 1: 16 X 16 Si:Bi AMCID Array Camera System Characteristics

Well Capacity	2×10^5 electrons
Read Noise[a]	< 600 electrons
Dark Current	200 electrons sec^{-1}
Quantum efficiency	$\lesssim$ 5%
Responsivity	0.5 Amp W^{-1} (high background)
Noise Equivalent Power[b]	$4 \times 10^{-17} WHz^{-1/2}$ (zero background)
Observational NEFD	0.1 Jy per pixel in 60 seconds
Optical Frequency Response	200 Hz (@ 10^9 photons $sec^{-1} pixel^{-1}$)
	= 25 Hz (@ 10^7 " " ")
Maximum Frame Rate	800 Hz

[a] System noise limited. 150 electrons detector read noise measured by Ames (2 x 64 Si:Bi array), <100 electrons for this family of detectors estimated by Aerojet.

[b] Considering noise derived from dark current only (zero background).

Table 2: Adopted Standard Star Flux Densities

Star	Flux density (Janskys) 8.3 μm	12.4 μm
β Peg	551.7	282.1
β And	372.6	181.0

III. OBSERVATIONS

a) Experimental Configuration

The Galactic Center observations were made on the nights of 1983 August 16 and 17 at the 3-meter NASA Infrared Telescope Facility (IRTF) at Mauna Kea, Hawaii. A total of thirty individual 60 or 120 second exposures at twelve positions around IRS 16 were obtained at effective wavelengths 8.3 and 12.4μm, with bandwidths of 0.8 and 0.3μm respectively. Additional observations were made at 9.7μm which were not sufficiently extensive for analysis here. Beam switching was 30 arcsec to the south at 10 Hz. The reference beam was examined for the presence of compact infrared sources, and in the few cases in which one was found it was removed during image processing.

The optical plate scale at the IRTF is 0.78 arcsec per detector pixel. The theoretical diffraction limited diameter of a point source at 8.3 and 12.4μm is λ/D = 0.57 and 0.85 arcsec (FWHM), respectively. The convolution of the diffraction disc with the array pixel profile results in an ideal instrumental profile of about 1.0 arcsec, neglecting cross-talk effects and seeing. Visual seeing was about 0.5 arcsec on both nights. The observed beam profile (FWHM) at both wavelengths was 1.3 arcsec in declination and 2.3 arcsec in right ascension, including tracking and infrared focus errors, determined from images of β Peg. The degradation in right ascension is due to non-optimal array guard band bias level (used to limit detector cross-talk).

b) Array Detector Calibration

Absolute flux calibration was based on observations of infrared standard stars β Peg and β And. The flux densities adopted for these stars in our two bands are given in Table 2, interpolated from fluxes published by Low and Rieke (1974), Gehrz, Hackwell, and Jones (1974), Forrest (1975), and Tokunaga (1984). The absolute photometric accuracy of the Galactic Center observations is estimated to be ± 10%. An atmospheric extinction correction ranging from 1.1 to 1.4 has been applied to each Galactic Center image, based on standard star data and the results of Low and Rieke (1974).

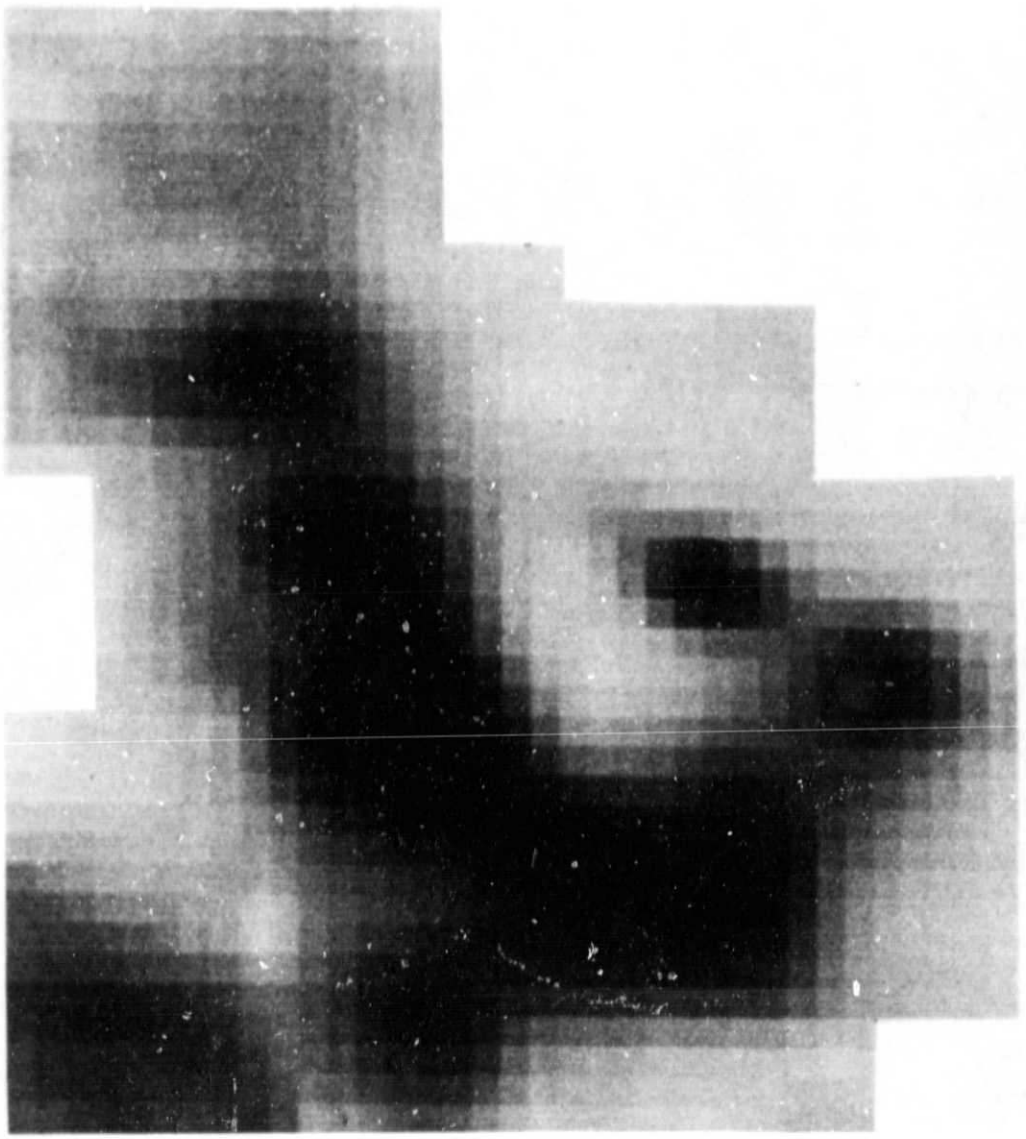

Figure 1: Composite 12.4 μm image of the Galactic Center region made up of a mosiac of averaged 16 x 16 pixel array exposures, illustrating the scale and nature of the processed array detector data from which the smoothed images in Figure 2 and contour maps in Figure 3 were generated. Each pixel is 0.8 arcsec square, corresponding to an array detector element. The detector optics were chosen so that two 0.8 arcsec detector pixels were approximately matched the diffraction limit (diameter FWHM) of the IRTF, as described in the text. The irregular borders indicate the extent of the region mapped. Darker regions indicate higher surface brightnesses.

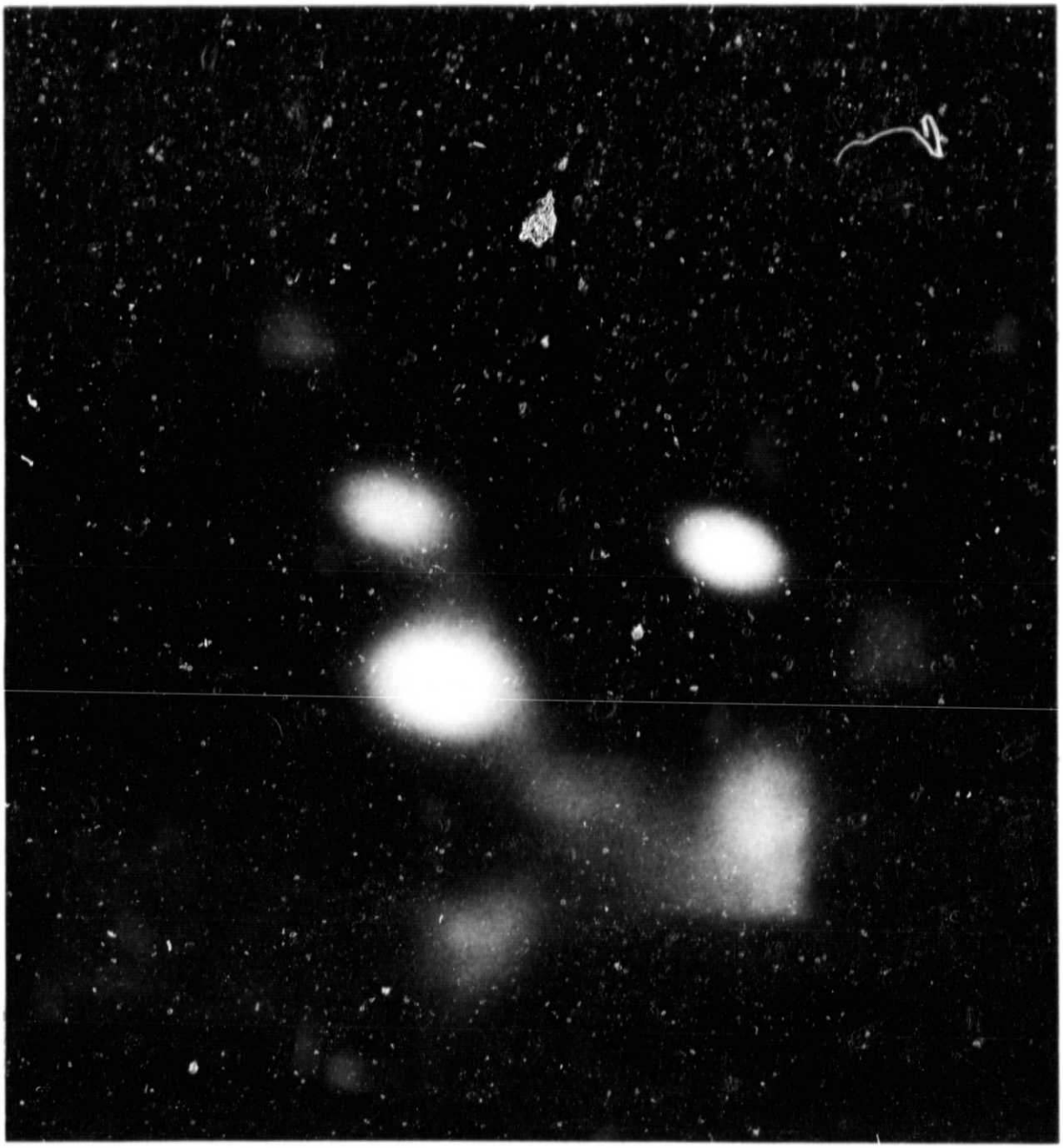

Figure 2(a): Image of the Galactic Center complex covering a 30 x 30 arcsec field observed at 8.3μm with the Goddard Infrared Array Camera (smoothed intensity distribution). The observational beam profile was θ(FWHM) = 1.3 x 2.3 arcsec due to seeing, guiding and instrumental effects. All of the bright compact sources are resolved, as discussed in the text. See Figure 3 for source identifications, photometric calibration and positions.

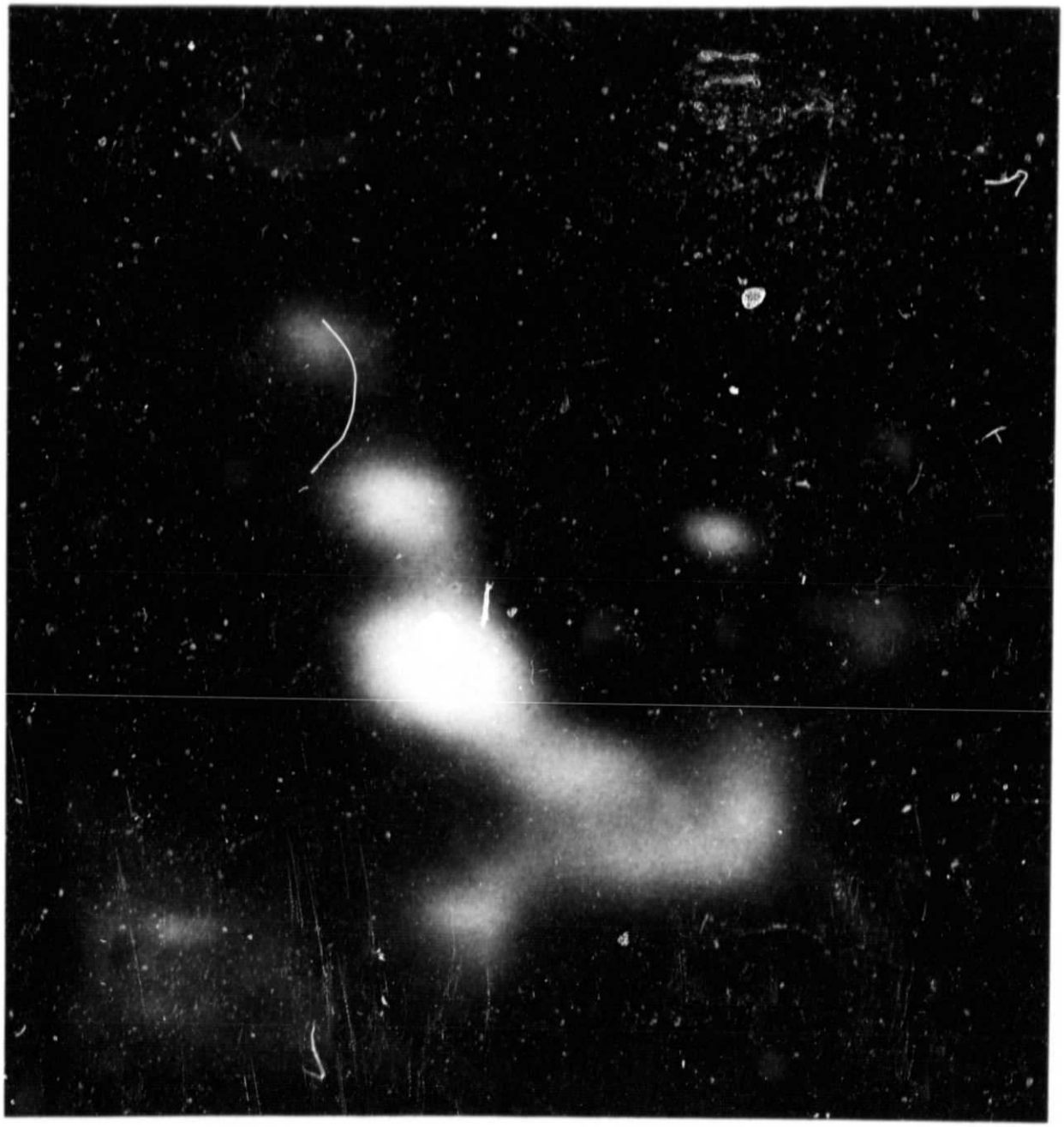

Figure 2(b): 12.4μm smoothed intensity distribution. As in Figure 2(a), the observational beam profile was θ(FWHM) = 1.3 x 2.3 arcsec, and all of the bright compact sources are resolved. See Figure 3 for source identifications, photometric calibration and positions.

Based on observations with this system in 1983 May and August, the 1σ noise equivalent flux density (NEFD) of the camera system during operation with typically 5% bandwidth filters was NEFD ≈ 0.1 Jy per pixel in a 60 second integration, the limit for extended sources. Since a point source image is spread over several detector pixels, the minimum noise equivalent point source flux density is about 2 Jy in 60 seconds (1 Jy = 10^{-26} W m^{-2} Hz^{-1}).

Flat-field correction ("gain") matrices were generated for each filter by integrating on blank sky fields at large and small airmasses. Gain matrices are found to be stable to within 5% throughout a night of observing. Flat-fielding is achieved by dividing the gain matrix into the image matrix. Relative position registration between partially overlapping images is determined with a cross-correlation algorithm which computes offsets to the nearest quarter pixel (0.2 arcsec).

IV. RESULTS

Figure 1 shows the 8.3μm processed array data in detector pixel format. Grey-scale images of the Galactic Center source complex at 8.3 and 12.4μm are presented in Figure 2, and contour maps calibrated in position and intensity at 8.3 and 12.4μm are shown in Figure 3. The positional calibration of the maps is based on the coordinates of IRS 7 given by Henry, DePoy, and Becklin (1984).

a) Emission Near the Nominal Galactic Center

None of the three components of IRS 16 (Storey and Allen 1983; Henry, DePoy and Becklin 1984) was detected at 8.3μm or 12.4μm, nor was any emission structure seen at the position of the nominal Galactic Center, Sgr A*, to a 3σ upper limit surface brightness of 0.5 Jy/arcsec^2. However, a new compact infrared source which we designate "IRS 21" was detected, which coincides to within the positional uncertainties with radio source #21 found by Brown, Johnston, and Lo (1981)[7] and seen by Lo and Claussen (1983) between IRS 1 and 2. The presence of IRS 21 can now be inferred from inspection of previous infrared observations which did not spatially resolve the source (Becklin and

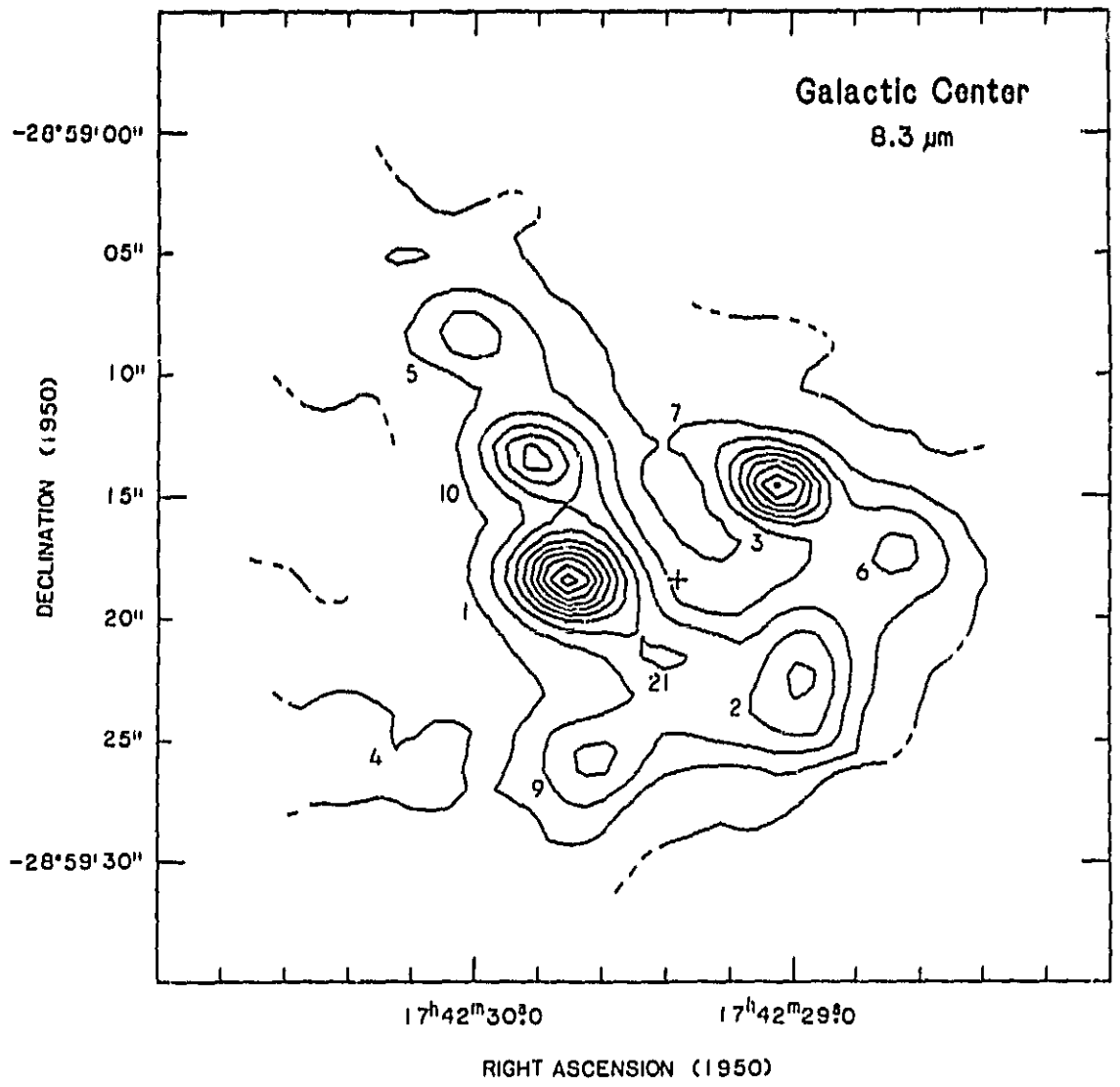

Figure 3(a): Calibrated surface brightness isophotes for the Galactic Center region at 8.3μm. The lowest contour plotted is 3σ above the noise level. Compact sources are labeled with their IRS numbers. The position for IRS 16(Center) and Sgr A* is shown by the cross. The contour interval is 0.61 Jy/arcsec^2, a 6σ increment. The peak 8.3μm brightness is 7.0 Jy/arcsec^2 at IRS 1.

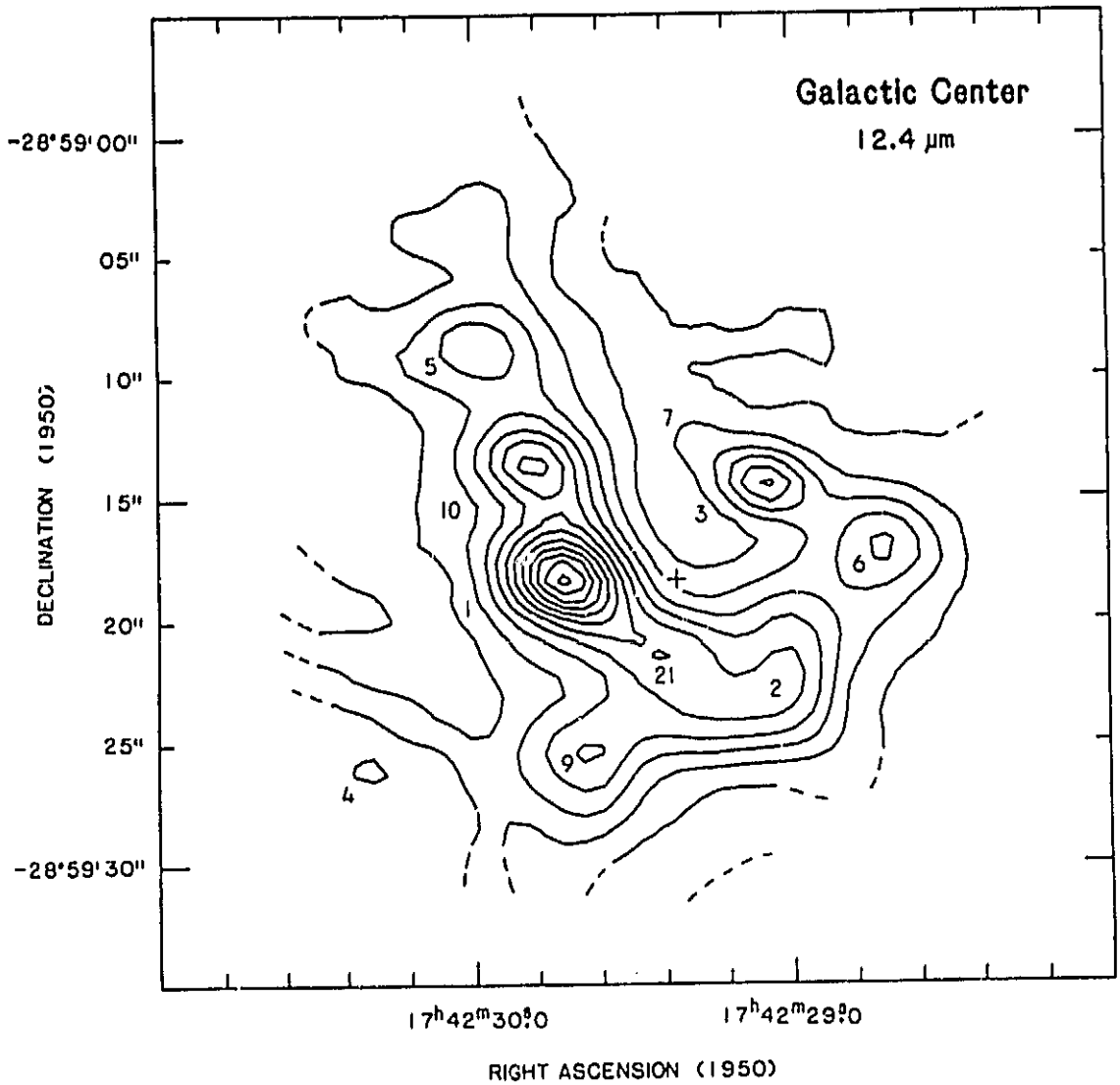

Figure 3(b): Galactic Center 12.4μm surface brightness distribution. The contour interval is 1.36 Jy/arcsec^2, a 6σ increment. Peak brightness is 16.9 Jy/arcsec^2 at the position of IRS 1. See Figure 3(a).

Neugebauer 1975; Becklin et al. 1978a; Rieke, Telesco, and Harper 1978). A discrete ionized gas cloud like those associated with the other IRS sources is present at the position of IRS 21 in the data of Lacy et al. (1980).

From our photometric images IRS 21 appears similar to the other ridge sources. Its 8.3μm/12.4μm color is similar to that of IRS 9, and the estimated ratio of 10μm to 5 GHz flux density is ∿ 300, well within the range observed by Brown, Johnston, and Lo (1981) for the other IRS objects. On the basis of these results there is nothing to distinguish IRS 21 from neighboring compact sources, other than a large velocity gradient across the radio source (Serabyn 1984).

b) Astrometry of the Source Complex

i) Source Positions

The array camera has an intrinsic capacity for high accuracy relative astrometry. Positions for the sources detected at 8.3 and 12.4μm are presented in Table 3. The tabulated values are averages derived from measurements on individual smoothed 16 x 16 pixel images. The systematic uncertainty in our determination of a source position within an individual array image is ∿ 0.25 arcsec (r.m.s.) for bright compact sources, and ∿ 0.4 arcsec for more extended objects. Including all sources of error, relative positions across the map are typically accurate to better than ± 0.5 arcsec.

Most source positions measured from the array images agree with previously published positions to within the uncertainties. Significant

---

[7] Brown, Johnston, and Lo (1981) named this radio source "#21" following the numbering sequence used by Becklin and Neugebauer (1975) for IRS sources, although no infrared source had been detected at that position. We assign "IRS 21" to the new compact 10μm source, since it coincides in position with radio source #21.

Table 3: Observed Positions of IRS Objects[c]

IRS Source	8.3μm		12.4μm	
	RA (1950)	DEC	RA (1950)	DEC
1(w)	$17^h42^m29^s.68$	$-28^o59'18''.2$	$17^h42^m29^s.68$	$-28^o59'18''.3$
2	17 42 28.96	-28 59 22.2	17 42 28.99	-28 59 22.7
3	17 42 29.03	-28 59 14.5	17 42 29.05	-28 59 14.5
4			17 42 30.28	-28 59 26.0
5	17 42 29.98	-28 59 08.3	17 42 29.94	-28 59 08.8
6	17 42 28.67	-28 59 17.3	17 42 28.71	-28 59 17.1
7	17 42 29.26	-28 59 12.6	17 42 29.26	-28 59 12.6
9	17 42 29.60	-28 59 25.4	17 42 29.62	-28 59 25.4
10	17 42 29.78	-28 59 13.3	17 42 29.77	-28 59 13.7
21	17 42 29.38	-28 59 21.5	17 42 29.38	-28 59 21.4

[c]Absolute positions are based on the corrected position of IRS 7 determined by Henry, Depoy and Becklin (1984): $\alpha = 17^h42^m29^s.34$, $\delta = -28^o59'12''.9$. Positions of other sources relative to IRS 7 are determined from individual smoothed images to an accuracy of 0.2 arcsec in R.A. and DEC. IRS 7 is not depicted clearly in Figures 2 and 4, which are comprised of smoothed co-added frames. The average 1σ statistical uncertainty (excluding systematic errors) is $\Delta\alpha = \pm 0^s.01$, $\Delta\delta \sim \pm 0''.2$.

differences occur only for the extended sources IRS 2, 4, 6, and 9; in these cases the position may be wavelength dependent. The best published 10 μm source positions relative to IRS 7 (Becklin and Neugebauer 1975; Becklin et al. 1978a) are uniformly about 0.5" E-SE of our positions, suggesting that their position for IRS 7 was slightly in error.

Our high resolution astrometry establishes that the 10 μm source IRS 1 is in fact the western component, IRS 1(W), of the 2 μm double source resolved by Storey and Allen (1983) and Bailey, Hough, and Axon (1984). IRS 1(W) is the redder of the two components, and has associated Brackett γ emission (Storey and Allen 1983).

The distribution of infrared and radio continuum emission in the Galactic Center is strikingly similar. The extended 10 μm curved ridge of emission corresponds exactly with the "northern arm" and "ionized bar" of radio continuum emission. These large scale structures and the numerous compact infrared sources (Figure 3) are prominent in the high resolution radio continuum maps of Brown, Johnston, and Lo (1981), Ekers et al. (1983) and Lo and Claussen (1983). The only significant positional discrepancy is for the extended source IRS 6, which lies closer to IRS 16 at radio wavelengths than it does at 2 or 10 μm. IRS 3 and 7 are stars which do not appear in the radio maps, c.f. §IV(b).

ii) Source Sizes

Source diameters were measured accurately for the most distinct compact sources. The observed beam profile was deconvolved from the observed source profiles to yield the effective source dimensions, given in Table 4. To within the uncertainties, these sizes are consistent with the typically 0.1 - 0.3 pc diameters of the associated ionized gas clouds studied by Lacy et al. (1980).

IRS 1, 5, 6, 9, and 10 all appear resolved in our images. The extended low surface brightness source IRS 4 is clearly larger than IRS 6 and 9, and appears as a double in Lo and Claussen's (1983) radio continuum map. IRS 3

TABLE 4 — Observed and Deconvolved Source Diameters

Source	8.3μm		12.4μm	
	Observed Diameter (FWHM)	Deconvolved Source Size (FWHM)[d]	Observed Diameter (FWHM)	Deconvolved Source Size (FWHM)[d]
IRS 1(W)	2.7"	2.3"	3.5"	3.2"
3	2.1	1.6	2.1	1.6
5	3.6	3.3	4.6	4.4
6	5.8	5.6	4.7	4.5
9	5.2	5.0	5.6	5.4
10	3.1	2.8	4.4	4.2

[d] 1σ (r.m.s.) uncertainty $\sim$ 0.2 arcsec.

has previously been reported to be unresolved in a 1.5 arcsec beam (Rieke, Telesco, and Harper 1978) and to have a size < 1 arcsec (Rieke 1978). We derive a size of 1.6 ± 0.2 arcsec (FWHM) for IRS 3 at both 8.3 and 12.4μm.

c) Color Temperatures

Most of the strong compact 10μm sources in the Galactic Center region are not prominent features in the derived color temperature distribution (Figure 4) calculated from the ratio of 8.3μm/12.4μm emission (Figure 3). We find the curved ridge of 10μm emission corresponding to the northern arm and ionized bar to be a region of almost constant temperature, and cooler than the surrounding diffuse material.

These calculations have assumed blackbody grain emission. We have not attempted to model grain parameters, therefore, the derived color temperatures may not be accurate physical temperatures. The images were corrected for interstellar extinction prior to computing color temperatures, based on studies of extinction to the Galactic Center between 1 and 20μm (Becklin *et al.* 1978 and Rieke and Lebofsky 1985). The adopted values of extinction at 8.3 and 12.4μm are 1.1 ± 0.2 and 1.0 ± 0.2 mag, respectively.

On the basis of the color temperature map (Figure 4), the IRS sources may be divided into three groups. IRS 1, 5, and 10 have color temperatures of T_c ∿290K, and are embedded in the cooler diffuse component of the ∿250K northern arm. IRS 2, 9, and 21 (T_c ∿ 250 - 290K) in the ionized bar are indistinguishable from the background, and IRS 4 and 6 (T_c < 260K) appear to be cooler than their surroundings.

IRS 3 and IRS 7 are the hottest features in the map, with $T_c \gtrsim$ 400K. IRS 3 is believed to be a dust-shrouded supergiant star (Rieke, Telesco, and Harper 1978; Becklin *et al.* 1978a; and Rieke 1978), which is also likely for IRS 7 (c.f. Becklin and Neugebauer 1975). Neither source appears in radio continuum maps. Both objects should probably be considered independently of the rest of the 10μm complex, as made evident by the emission optical depth map presented in the following section.

The color temperature results presented in Figure 4 differ substantially from the results of Rieke and Lebofsky (1982), which predicted a temperature peak at the position of each of the compact 10μm sources. However, their model was based on 5, 10, and 56μm data acquired by different investigators with widely differing spatial resolution. Our color temperatures are uniformly about 50K higher than those reported by Aitken, Allen, and Roche (1982) based on observations at 10.5 and 12.5μm. This discrepancy is not significant. The conclusions drawn in subsequent sections are not sensitive to the absolute temperatures since our interpretation is based on the relative temperature structure of the region.

The temperature contrast between IRS 1, 5 and 10 and the extended emission is at least 5 σ, derived from the statistical uncertainties of the observed intensities (1σ = 5K at the IRS sources). In the ionized bar, however, IRS 4 or IRS 6 are nearly the same temperature as the surrounding material. The intensities are less well-determined in the outer regions of the maps where fewer individual images were taken, and spatial coverage near IRS 4 and 6 is incomplete. Due to these uncertainties, the color temperature results are best understood as indicating that, unlike the IRS sources in the northern arm, the sources in the ionized bar are not significantly hotter than their surroundings. The absence of a temperature peak at IRS 21 is noteworthy since this object is situated close to the apparent terminus of the paths of infall toward the nucleus proposed by Lo and Claussen (1983).

The color temperature results show that temperatures away from the arm and bar are generally higher than temperatures within the complex of 10μm sources, although this result derives from data in regions with the lowest signal/noise. The significant implication of these results is that the 10μm IRS sources are not dominant factors in the large scale temperature structure of the region.

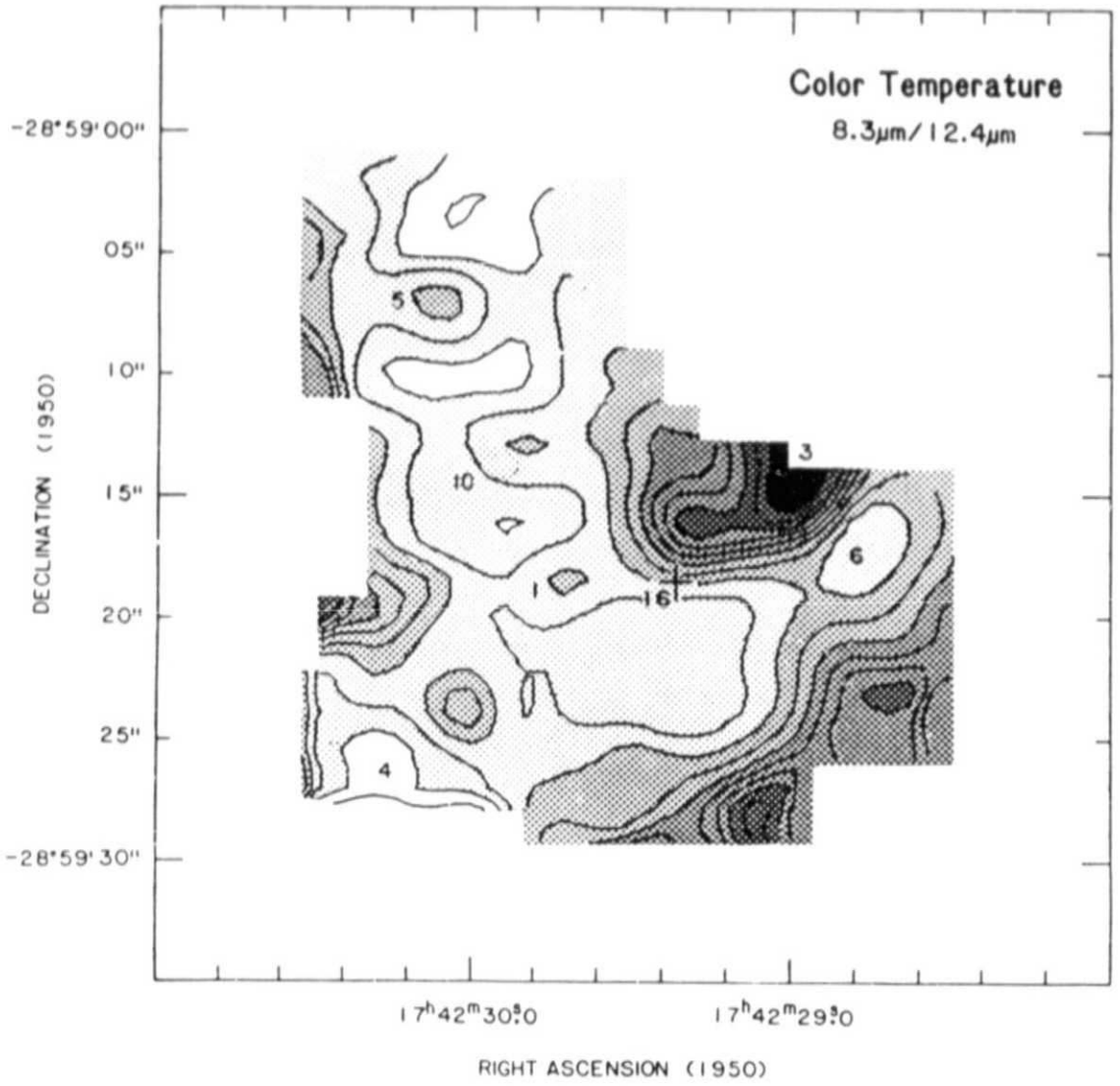

Figure 4: Derived color temperature for the Galactic Center source complex, calculated from the 8.3μm/12.4μm image ratio assuming blackbody spectra. Darker shades are higher temperature. The position of Sgr A* and IRS 16(Center) is shown by the cross. The lowest temperature contour is T_c = 220K; contours are plotted at 20K intervals (1σ = 5K in regions of high infrared surface brightness). The peak color temperature T_c = 400K occurs at IRS 3. IRS 1, 5 and 10 are each 290K, and IRS 6 is 260K. Higher color temperatures based on lower signal to noise data in the weakest regions may not be physically significant (see Figure 3).

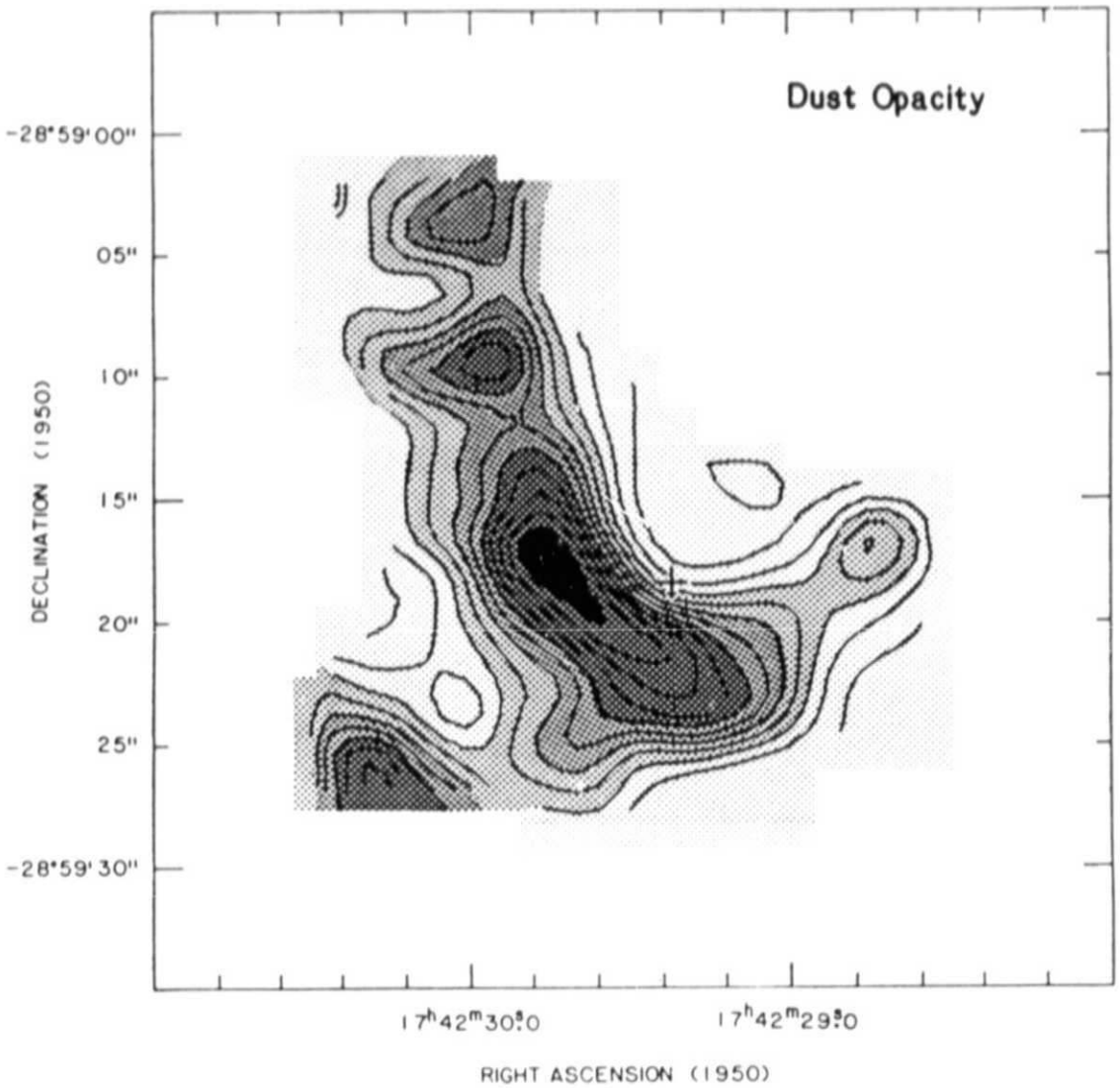

Figure 5: Derived opacity of warm dust grains giving rise to the observed Galactic Center 8.3μm emission. Darker shades are high opacity. The position of IRS 16(Center) is shown by the cross. The lowest contour plotted is $\tau = 5.0 \times 10^{-4}$, and the contour interval is $\tau = 5.0 \times 10^{-4}$. The peak opacity $\tau = 5.6 \times 10^{-3}$ occurs at IRS 1.

d) Dust Opacity

The opacity distribution of warm emitting dust grains (Figure 5) has been calculated from the observed intensity and derived color temperature distributions. We assume that 8 - 13μm emission arises from warm grains within the central few parsecs of the Galactic Center, and that interstellar extinction is uniform with the wavelength dependence derived by Rieke and Lebofsky (1985). The radiative transfer equation is solved for the emission optical depth of the warm grains, yielding a first order direct estimate of the relative dust density in the central parsec of the galaxy.

The observed 8 - 13μm emission from the Galactic Center source complex is optically thin everywhere with a typical value of $\tau = (2 \pm 1) \times 10^{-3}$. Thus, infrared radiation is detected with equal efficiency throughout the central few parsecs of the Galaxy. The northern arm and ionized bar are clearly seen as dust density enhancements. The opacity is greatest near all of the 10μm objects, and falls off steeply away from them. Even relatively weak sources like IRS 4, 5, and 6 are strong density peaks. The lowest densities in Figure 5 occur in the region of apparently enhanced color temperature off the ridge between IRS 1 and IRS 3. IRS 3 itself is barely discernible as a density feature, a manifestation of its relatively compact circumstellar dust shell.

Because the 10μm emission is optically thin everywhere, we can estimate the dust mass in the 1.5 x 1.5 parsec region mapped. Following Hildebrand (1983), and assuming typical values of hot grain parameters such as those derived by Becklin *et al.* (1976) for the Orion trapezium region, a total mass of $M \sim 0.05\ M_\odot$ is derived for the hot grains mapped with the array camera. The presence of a population of larger, cooler grains observed at far infrared wavelengths would contribute an order of magnitude additional mass, for a total dust mass of about $0.5\ M_\odot$. Using the standard dust/gas mass ratio (0.01), we derive an ionized gas mass of $\sim 50\ M_\odot$ in the central parsec, consistent with the results of VLA observations of the region by Lo and Claussen (1983). Since Harris *et al.* (1985) and Genzel *et al.* (1985) deduce a mass of $\sim 10^4\ M_\odot$ in the $r \sim 2$ pc ring, our results support the contention of Becklin, Gatley, and Werner (1982) that the volume immediately surrounding the Galactic Center is significantly depleted in gas and dust.

V. DISCUSSION

a) The Complex Nature of the Central Parsec

The derived color temperature and emission optical depth maps presented here offer further evidence for multiple, distinct structures near the Galactic Center. The IRS sources in the northern arm differ in temperature, density and size from their counterparts in the ionized bar. IRS 1, 5, and 10 are equal in temperature, and significantly warmer than the diffuse environment in which they are embedded. Between the IRS sources, the northern arm is cooler than the diffuse part of the ionized bar. The sources in the bar are not prominent as temperature peaks, suggesting the possibility that the heating mechanisms in the two features are different, as discussed in §V(b).

The high resolution radio continuum map of Ekers *et al.* (1983) revealed what appeared to be a spiral distribution of ionized gas centered near the unusual point source Sgr A*. Lo and Claussen (1983) re-examined earlier dynamical data to ascertain that the radio spiral was not a single feature, but consisted of two or more distinct, coherent flows around and toward (or away from) the galactic nucleus. By observing the [NeII] 12.8μm fine-structure line throughout the ionized gas in the radio continuum features, Serabyn and Lacy (1985) established that the material in the northern arm is apparently flowing in an eccentric orbit about a concentrated mass of 3-4 x 10^6 $M_\odot$. These and other data, such as the CO observations of Harris *et al.* (1984) and the far-infrared atomic and molecular line observations of Genzel *et al.* (1985), also chart a flow at radius $\sim$ 2 pc corresponding to the western arc which lies outside the region mapped with the infrared array camera.

It has also become apparent that the material in the ionized bar between IRS 4 and 6 is distinct from that in the northern arm in several ways. Rather than displaying a smooth variation of velocity with position, as is seen in the northern arm and western arc (Lacy *et al.* 1980; Serabyn and Lacy 1985), the bar has a complicated velocity structure with positive velocities to the SE near IRS 4, negative velocities to the NW near IRS 6, and an increasing velocity dispersion toward the center of the bar near IRS 21. This behavior

led Lo and Claussen (1983) to suggest that the bar consists of two independent features falling toward or being ejected from the nucleus.

Neglecting the peaks at the positions of the compact sources, the emission optical depth steadily increases from north of IRS 5 down along the northern arm toward a maximum near IRS 1 and 21. In the context of [NeII] observations showing a continuous decrease in velocity along the arm from north to south (Serabyn and Lacy 1985), we interpret this result as confirmation that IRS 1, 5, and 10 are local condensations, embedded within a continuous flow of material around the Galactic Center.

b) Heating Mechanism for the IRS Objects

Previous workers have identified the Galactic Center 10μm sources as local temperature peaks (Rieke and Lebofsky 1982; Aitken, Allen and Roche 1982; Rieke, Telesco, and Harper 1978; and Becklin et al. 1978a), and the presence of a compact infrared source at a local peak in color temperature has been frequently cited as evidence for internal heating by an embedded luminosity source, possibly a recently formed star. It has been suggested that the near infrared emission from these sources arises from a central star, and the 10μm emission from the surrounding dust cloud (Lebofsky et al. 1982).

In the high resolution, spatially calibrated array camera images presented here, only the IRS sources in the northern arm appear as local temperature maxima. The others (not including the stars IRS 3 and 7) do not exhibit the temperature structure expected of objects containing embedded luminosity sources. The maps of derived color temperature and dust emission optical depth imply that the 10μm complex is bright not because it is self luminous but because it represents a significant enhancement in dust density.

Even the IRS sources in the northern arm may not be heated internally. The ionic abundances observed in the region have been explained by a radiation field characteristic of stars with $T_{eff} < 35{,}000K$ (Lacy et al. 1980). Although the power available for direct grain heating greatly exceeds the contribution due to resonant trapping of Lyman α photons, Ly α trapping could

provide an additional source of grain heating where the dust density is substantially peaked, raising the temperature above that of the surrounding area whether or not there is a luminosity source within the clump (Gatley 1982). Thus temperature peaks can be generated by external heating of the dust clouds.

An increase in source size with the wavelength of observation has been noted for some of the IRS objects in the central parsec of the galaxy as additional evidence of internal heating (Rieke, Telesco, and Harper 1978; Rieke 1978). However, our source diameter results (Table 4) reflect only a marginal increase in size between 8.3 and 12.4μm for three sources (IRS 1, 5, and 10) and may also indicate the increased contribution of Ly α trapping in the dense core of each object. We cannot rule out the possibility that IRS 1, 5, and 10 contain embedded luminosity sources, but they are not required to fit our observations. Conversely, our color temperature and dust opacity results suggest that IRS 2, 4, 6, 9 and 21 do not contain embedded stars.

c) Luminosity Sources

If the 10μm complex is not heated primarily by luminosity sources embedded within the IRS objects, it is interesting to consider how the dust in the central parsec might be heated to temperatures exceeding 250K. Becklin, Gatley, and Werner (1982) established on the basis of far-infrared observations that some $1 - 3 \times 10^7$ L_o are emitted in the galactic nucleus, and Henry, DePoy, and Becklin (1984) demonstrated that nearly all of this luminosity may be attributable to IRS 16/Sgr A*. Following Scoville and Kwan (1976), we calculate that grain temperatures in excess of 300K can be obtained assuming grain properties as in Section IV(c) and a single source of 2×10^7 L_o at the center of a distribution of grains 2 pc from the source. Thus, it appears that the temperature structure deduced from our new 10μm images is consistent with the presence of a central engine at the galactic nucleus. Gatley (1982) has shown that the 20μm/34μm color temperature distribution is symmetric about the position of IRS 16. Additional high-resolution mapping with more extensive spatial coverage could establish the relationship between the central engine and the heating of the features observed at infrared and radio continuum wavelengths.

VI. SUMMARY

We have presented new intensity, color temperature, and emission optical depth maps of the Galactic Center obtained with a 8-13μm array camera system. These data have been examined in the context of a model for a dominant central luminosity source at the galactic nucleus, surrounded by several continuous flows of ionized gas and dust. The principal conclusions are:

1) The "northern arm" and "ionized bar" are not conspicuous color temperature features. These large-scale structures are nearly constant in temperature and cooler than the material away from the ridge of 8 - 13μm emission.

2) IRS 1, 5 and 10 are slightly warmer than the surrounding northern arm structure, and could be partially self-luminous. However, IRS 2, 4, 6, 9, and 21 are not distinguishable in color temperature from the surrounding extended material in the bar structure.

3) The color temperature distribution suggests that the infrared source complex is heated externally, possibly by a dominant central luminosity source.

4) The total dust mass density we derive in the central parsec is much smaller than the density in the ~ 2 pc radius ring encircling the nucleus. The most likely candidate for the central engine, IRS 16/Sgr A*, was not detected in these observations. These results are interpreted as further evidence for the lower density of interstellar material immediately surrounding the Galactic Center.

Considered in the context of previous observations, the derived dust opacity and color temperature distributions are consistent with the predictions of "central engine" models for the energetics of the Galactic Center. These results do not determine the nature of this luminosity source, but they do indicate that internal heating is not apparent, and that a significant fraction of the material in the complex is externally heated. Successful models for the energetics of the inner few parsecs should, therefore, address a central source of luminosity at the Galactic Center.

ACKNOWLEDGMENTS

We thank Chris Parry and Aerojet ElectroSystems Company for providing AMCID array detectors for the Goddard Array Camera. Harvey Moseley developed the camera dewar design and has provided many useful suggestions for observational and technical procedures. Jeffrey Bowser and Ramesh Sinha of Systrems and Applied Research Corp. have contributed actively to the development of the camera system software, much of which is based on software originally written by Gordon Chin. We are grateful to Michael Hauser and Michael Mumma for their support of this project, and to Richard Capps, Eric Becklin, and the staff of the NASA Infrared Telescope Facility. We thank Al Harper, Steve Willner, and Dan Watson for helpful comments and suggestions. Doug MacDonald and Thomas Stephenson assisted with image processing at the Center for Astrophysics. The array camera was supported by NASA OSS 188-41-55-08, NASA OAST 506-54-21, the NASA/Goddard Directors' Discretionary Fund, a NASA Core Grant to Harvard University, and Steward Observatory.

References

Aitken, D. K., Allen, M. C., and Roche, P. F. 1982, in The Galactic Center, ed. G. R. Riegler and R. D. Blandford, AIP Conf. Proc. No. 83, p. 67.

Bailey, J., Hough, J. H., and Axon, D. J. 1984, M.N.R.A.S., 208, 661.

Balick, B. and Brown, R. L. 1974, Ap. J., 194, 265.

Becklin, E. E., Gatley, I., and Werner, M. W. 1982, Ap. J., 258, 135.

Becklin, E. E., Matthews, K., Neugebauer, G. and Willner, S. P. 1978a, Ap. J., 219, 121.

Becklin, E. E., Matthews, K., Neugebauer, G. and Willner, S. P. 1978b, Ap. J., 220, 831.

Becklin, E. E. and Neugebauer, G. 1975, Ap. J. (Letters), 200, L71.

Brown, R. L., Johnston, K. J., and Lo, K. Y. 1981, Ap. J., 250, 155.

Brown, R. L. and Liszt, H. 1984, Ann. Rev. Astr. Ap., 22, 223.

Crawford, M. K., Genzel, R., Harris, A. I., Jaffe, D. T., Lacy, J. H., Lugten, J. B., Serabyn, E., and Townes, C. H. 1985, Nature, 315, 467.

Ekers, R. D., van Gorkom, J. H., Schwarz, U. J., and Goss, W. M. 1983, Astr. Ap., 122, 143.

Forrest, W. F. 1975, Ph.D. thesis, U.C. San Diego.

Gatley, I. 1982, in The Galactic Center, ed. G. R. Riegler and R. D. Blandford, AIP Conference Proceedings No. 83, p. 25.

Gatley, I. and Becklin, E. E. 1981, in Infrared Astronomy, IAU Symposium 96, ed. C. G. Wynn-Williams and D. P. Cruikshank, Dordrecht: D. Riedel Publishing Co., p. 281.

Gatley, I., Jones, T. J., Hyland, A. R., Beattie, D. H., and Lee, T. J. 1984, M.N.R.A.S., 210, 565.

Geballe, T. R., Krisciunas, K., Lee, T. J., Gatley, I., Wade, R., Duncan, W. D., Garden, R., and Becklin, E. E. 1984, Ap. J., 284, 118.

Gehrz, R. D., Hackwell, J. A., and Jones, T. W. 1974, Ap. J., 191, 675.

Genzel, R., Watson, D. M., Crawford, M. K., and Townes, C. H. 1985, Ap.J., (in press).

Hall, D. N. B., Kleinmann, S. G., and Scoville, N. Z. 1982, Ap. J. (Letters), 262, L53.

Henry, J. P., DePoy, D. L., Becklin, E. E. 1984, Ap. J. (Letters), 285, L27.

Hildebrand, R. H. 1983, QJRAS, 24, 267.

Krisciunas, K., Geballe, T. R., and Wade, R. 1984, B.A.A.S., 16, 980.

Lacy, J. H., Townes, C. H., Geballe, T. R., and Hollenbach, D. J. 1980, Ap. J., 241, 132.

Lamb, G. M., Gezari, D. Y., Shu, P., Tresch-Fienberg, R., Fazio, G. G., Hoffmann, W. F., and McCreight, C. R., 1984, Proc. S.P.I.E., 445, 113.

Lebofsky, M. J., Rieke, G. H., Deshpande, M. R., and Kemp, J. C. 1982, Ap. J., 263, 672.

Lebofsky, M. J., Rieke, G. H., and Tokunaga, A. T. 1982, Ap. J., 263, 736.

Lingenfelter, R. E. and Ramaty, R. 1982, in The Galactic Center, ed. G. R. Riegler and R. D. Blandford, AIP Conference Proceedings No. 83, p. 148.

Lo, K.-Y. 1982, in The Galactic Center, ed. G. R. Riegler and R. D. Blandford, AIP Conference Proceedings No. 83, p. 1.

Lo, K.-Y., and Claussen, M. J., 1983, Nature, 306, 647.

Low, F. J. and Rieke, G. H. 1974, in Methods of Experimental Physics, ed. N. P. Carleton, 12, Part A, p. 415.

McCreight, C. R. and Goebel, J. H. 1981, Appl. Optics, 20, 3189.

McKelvey, M. E., McCreight, C. R., Goebel, J. H., Reeves, A. A. 1985, NASA TM #86667 (submitted to Appl. Optics).

Parry, C. M. 1980, Proc. S.P.I.E., 244, 2.

Parry, C. M. 1983, in Proc. Infrared Detector Technology Workshop, NASA Ames Research Center, ed. C. R. McCreight.

Rieke, G. H. 1978, in Infrared Astronomy, NATO Advanced Study Institute, ed. G. Setti and G. G. Fazio, Dordrecht: D. Reidel Publ. Co., p. 159.

Rieke, G. H. and Lebofsky, M. J. 1982, in The Galactic Center, ed. G. R. Riegler and R. D. Blandford, AIP Conference Proceedings No. 83, p. 194.

Rieke, G. H. and Lebofsky, M. J. 1985, Ap. J., 288, 618.

Rieke, G. H. and Low, F. J. 1973, Ap. J., 184, 415.

Rieke, G. H., Telesco, C. M., and Harper, D. A. 1978, Ap. J., 220, 556.

Scoville, N. Z. and Kwan, J. 1976, Ap. J., 206, 718.

Serabyn, E. 1984, Ph.D. Thesis, U.C. (Berkley) .

Serabyn, E. and Lacy, J. H. 1985, Ap. J., in press.

Storey, J. W. V. and Allen, D. A. 1983, M.N.R.A.S., 204, 1153.

Tokunaga, A. T. 1984, A. J., 89, 172.

Watson, M. G., Willingale, R., Grindlay, J. E., and Hertz, P. 1981, Ap. J., 250, 142.

D. Y. GEZARI, G. M. LAMB, AND P. SHU: NASA Goddard Space Flight Center, Code 697, Greenbelt, MD 20771.

G. G. FAZIO AND R. TRESCH-FIENBERG: Harvard-Smithsonian Center for Astrophysics, 60 Garden Street, Cambridge, MA 02138.

I. GATLEY: United Kingdom Infrared Telescope, 900 Leilani Street, Hilo, HI 96720.

W. F. HOFFMANN: Steward Observatory, University of Arizona, Tucson, AZ 85721.

C. R. McCREIGHT: NASA/Ames Research Center, Mail Stop 244-7, Moffett Field, CA 94035.

BIBLIOGRAPHIC DATA SHEET

1. Report No. NASA TM -86225	2. Government Accession No.	3. Recipient's Catalog No.
4. Title and Subtitle 8.3 AND 12.4 MICRON IMAGING OF THE GALACTIC CENTER SOURCE COMPLEX WITH THE GODDARD INFRARED ARRAY CAMERA		5. Report Date JULY 1985 6. Performing Organization Code 697
7. Author(s) D.Y. Gezari, R. Tresch-Fienberg, G. G. Fazio, W.F. Hoffmann, I. Gatley, G. Lamb, P. Shu, and C. McCreight		8. Performing Organization Report No.
9. Performing Organization Name and Address NASA/Goddard Space Flight Center Space & Earth Sciences Directorate Laboratory for Extraterrestrial Physics Infrared Astrophysics Branch		10. Work Unit No. 11. Contract or Grant No. 13. Type of Report and Period Covered Technical Memorandum
12. Sponsoring Agency Name and Address		14. Sponsoring Agency Code

15. Supplementary Notes

To be published in the Astrophysical Journal (Dec. 15, 1985)

16. Abstract

A 30 x 30 arcsec field at the Galactic Center (1.5 x 1.5 parsec) has been mapped at 8.3μm and 12.4μm with high spatial resolution and accurate relative astrometry, using the 16 x 16 Si:Bi AMCID Goddard infrared array camera. The design and performance of the array camera detector electronics system and image data processing techniques are discussed. Color temperature and dust opacity distributions derived from the spatially accurate images indicate that the compact infrared sources and the large scale ridge structure are bounded by warmer, more diffuse material. None of the objects appear to be heated appreciably by internal luminosity sources. These results are consistent with the model proposing that the complex is heated externally by a strong luminosity source at the Galactic Center, which dominates the energetics of the inner few parsecs of the galaxy.

17. Key Words (Selected by Author(s))	18. Distribution Statement
Infrared Array Detector Infrared Astronomy Galactic Center	Unclassified - unlimited 89 - Astronomy 33 - Electronics and Electronic Engineering

19. Security Classif. (of this report)	20. Security Classif. (of this page)	21. No. of Pages	22. Price*
UNCLASSIFIED	UNCLASSIFIED	32	

*For sale by the National Technical Information Service, Springfield, Virginia 22161

GSFC 25-44 (10/77)